A Stable Polyoxometalate-Pillared Metal-Organic Framework for Proton-Conducting and Colorimetric Biosensing

ARTICLE *in* CHEMISTRY - A EUROPEAN JOURNAL · JULY 2015

Impact Factor: 5.73 · DOI: 10.1002/chem.201501515 · Source: PubMed

7 AUTHORS, INCLUDING:

Chao Qin
Nanjing Medical University
262 PUBLICATIONS **6,157** CITATIONS
SEE PROFILE

Wei-Chao Chen
Northeast Normal University
9 PUBLICATIONS **41** CITATIONS
SEE PROFILE

ChemPubSoc Europe

DOI: 10.1002/chem.201501515

CHEMISTRY A European Journal Full Paper

Sensors

A Stable Polyoxometalate-Pillared Metal–Organic Framework for Proton-Conducting and Colorimetric Biosensing

En-Long Zhou, Chao Qin,* Peng Huang, Xin-Long Wang,* Wei-Chao Chen, Kui-Zhan Shao, and Zhong-Min Su*[a]

Abstract: A stable metal–organic framework pillared by Keggin-type polyoxometalate, $Cu_6(Trz)_{10}(H_2O)_4[H_2SiW_{12}O_{40}]\cdot 8H_2O$ (Trz = 1,2,4-triazole) (**1**), has been prepared under hydrothermal condition. The 2D layer structure with a 22-member ring was formed by Cu^{2+} ions, which are connected with each other via the Trz ligands on the *ab* plane. Thus, the 2D layers are further interconnected through Keggin polyoxoanions to generate a 3D porous network with a small 1D channel. Moreover, the presence of polyoxoanions make it exhibit selective adsorption of water and proton-conducting properties. Additionally it showed efficient intrinsic peroxidase-like activity, providing a simple and sensitive colorimetric assay to detect H_2O_2.

Introduction

Research interest has focused on the construction and characterization of versatile porous materials recently. Among the various porous materials, metal–organic frameworks (MOFs), as a new class of crystalline porous materials, have attracted great attention owing to their charming structural features and properties as well as their potential applications in catalysis, gas storage, separation, sensor and drug delivery.[1] Recently, the exciting new opportunities for MOFs have focused on proton-conducting materials, which can be obtained by introducing acidic and/or hydrophilic units or proton carriers into nanochannels.[2] However, the stability and water retention of most MOFs have been generally considered as an important indicator for their further modification and application.[3]

Polyoxometalates (POMs), as an excellent class of metal–oxide clusters with nanosize, adjustable compositions, oxygen-rich surface with strong coordination abilities and potential applications in catalysis, ion exchange, magnetism, and photochromic or electrochromic response, constitute promising building units for multifunctional materials.[4] The oxygen-rich surface of POMs also makes them promising as precursors linked by metal–organic groups to construct POM-based MOFs,[5] which has provided a new generation of microporous materials that combine the advantages of POM chemistry with the properties of MOF chemistry.[6] On one hand, the inlay of Keggin-type POMs into the ordered channels of MOFs would provide more hopping sites in the cavities and enhance the stabilities of MOFs. On the other hand, polyoxoanions are usually surrounded by plenty of water molecules through strong H-bonding affinity in the crystalline state, which might potentially construct the proton conducting pathways.

Recently, colorimetric biosensing has drawn intense attention in biological science and analytical chemistry owning to its simplicity, rapidity, cheapness and direct visual readout.[7] As a basis for this technique, colorimetric sensors that signal analyte interaction through a change in color are undoubtedly crucial for successful implementation. So far, enzyme-mimetic inorganic materials, such as Fe_3O_4, Au nanoparticles, ceria nanoparticles, graphene oxide, carbon nanotubes, carbon nanodots, etc., have been reported to exhibit catalytic activity similar to that found in natural peroxidases, and have been successfully employed as biosensors.[8] However, few studies on MOF-based biosensing,[9] especially for POM-based MOF materials, have been reported.

Herein, we report a novel POM-pillared MOF, $Cu_6(Trz)_{10}(H_2O)_4[H_2SiW_{12}O_{40}]\cdot 8H_2O$ (**1**) by employing the simple 1,2,4-triazole and copper ions in the presence of the $[SiW_{12}O_{40}]^{4-}$ anion through one-step self-assembly synthesis, which exhibits high stability, selective adsorption of water and proton-conductivity properties. Besides, compound **1** behaves as an efficient peroxidase mimic and quickly catalyzes the oxidation of 3,3′,5,5′-tetramethylbenzidine (TMB).

Results and Discussion

The reaction of $Cu(NO_3)_2\cdot 2H_2O$, Trz, $H_4SiW_{12}O_{40}$ and water under hydrothermal conditions generates blue block crystals of **1**. Single-crystal X-ray diffraction analysis shows that compound **1** crystallizes in the triclinic space group $P\bar{1}$. Six Cu^{2+}

[a] Dr. E.-L. Zhou, Prof. C. Qin, Dr. P. Huang, Prof. X.-L. Wang, Dr. W.-C. Chen, Dr. K.-Z. Shao, Prof. Z.-M. Su
Key Laboratory of Polyoxometalate Science of Ministry of Education
Institute of Functional Material Chemistry, Department of Chemistry
Northeast Normal University, Changchun, Jilin, 130024 (P. R. China)
E-mail: qinc703@nenu.edu.cn
wangxl824@nenu.edu.cn
zmsu@nenu.edu.cn

Supporting information for this article is available on the WWW under http://dx.doi.org/10.1002/chem.201501515.

ions, twelve Trz ligands, one $[H_2SiW_{12}O_{40}]^{2-}$ anion, and four coordination water molecules constitute the basic structural unit of **1**. All the Cu^{2+} ions adopt a six-coordinated environment in a distorted octahedral coordination geometry. Cu1 and Cu4 are connected by four nitrogen atoms from four different Trz ligands, one oxygen atom derived from water molecule and one terminal oxygen atom originating from the polyoxoanion. Cu2 and Cu5 are linked by five nitrogen atoms from four different Trz ligands and one terminal oxygen atom originating from the polyoxoanion. Cu3 and Cu6 are coordinated by four nitrogen atoms from four different Trz ligands and two terminal oxygen atoms originating from the two different polyoxoanions (Figure S1 in the Supporting Information). These Cu^{2+} ions are connected with each other via the Trz ligands to form a 2D layer structure on the *ab* plane (Figure 1 a). The $[H_2SiW_{12}O_{40}]^{2-}$ anion connects to eight Cu^{2+} ions via its six terminal oxygen atoms from the two opposite $\{W_3O_{13}\}$ fragments, two of which adopt a two-connected mode. Thus, the 2D layers are further interconnected through Keggin polyoxoanions to generate a single 3D porous network with ordered cube-like units of dimensions $14.92\times14.45\times11.92$ Å^3. The resulting 3D framework contains 1D channels with a size of 5.69×5.65 Å^2 along the *a* axis (Figure 1 b). PLATON analysis for **1** without the contribution of water showed that the effective free volume is 24.3 %.[10]

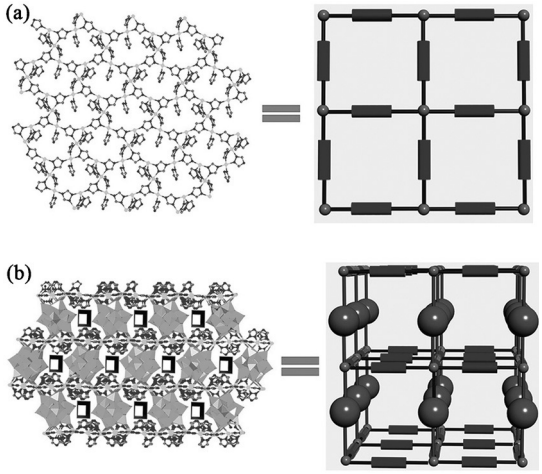

Figure 1. a) The 2D layer structure built by Cu^{2+} and Trz. b) The resulting 3D structure with a 1D channel along the *a* axis.

The IR spectrum and the powder X-ray diffraction (PXRD) pattern of the as-synthesized compound matched well with the simulated pattern, indicating its crystalline phase purity (Figures S2 and S3 in the Supporting Information). The TGA curve shows a weight loss of about 5.2 % from room temperature to 200 °C, which is related to the loss of coordinated water molecules and solvent water molecules. A further weight loss from 290 to 388 °C may be attributed to the decomposition of the framework (Figure S4 in the Supporting Information). Compound **1** was suspended in an aqueous solution at different pH values (pH 2, 11, 12; adjusted by HCl or NaOH) and in the common organic solvents (methanol and DMF). The mixtures were stirred at 80 °C for 24 h. Then, the solids were separated by centrifugation. The PXRD study shows that **1** can maintain structural integrity in aqueous solution over a wide pH range of 2 to 12, and in the common organic solvents (methanol, ethanol and DMF), which further indicated its high stability (Figure 2). We also measured the N_2 uptake for desolvated **1** at 77 K (Figure S5 in the Supporting Information). However, the desolvated **1** exhibited a low uptake for N_2, which may be attributed to the small channel (5.69×5.65 Å^2 without considering the van der Waals radius of the π-cloud of the Trz rings).

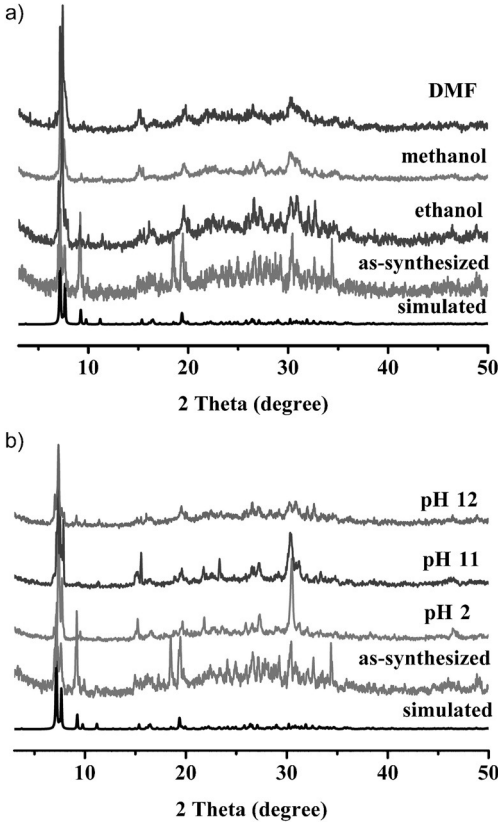

Figure 2. PXRD patterns for compound **1** after: a) soaking in different solvents, and b) soaking in solutions with different pH values.

Inspired by the excellent work by Mizuno and others,[11] the adsorption ability of **1** for water, methanol and ethanol due to its stability in water and common organic solvent were tested. The vapor adsorption isotherms for **1** were measured on desolvated sample. A PXRD comparison of **1** before and after adsorption experiments indicates that the integrity of the framework is retained during the adsorption process (Figure S6 in the Supporting Information). The TG data for desolvated **1** also indicate the complete removal of solvent molecules (Figure S7 in the Supporting Information). Figure 3 shows guest inclusion properties of **1** for water, methanol and ethanol at 298 K. For the water adsorption isotherm, the amount of water uptake increased monotonically with the vapor pressure and reached

approximately 50 cm^3 at $P/P_0 = 0.3$. The adsorption profile became steep at higher P/P_0 and ended with a maximum uptake of 118 $cm^3 g^{-1}$, equivalent to about 22 H_2O molecules per formula unit. On the other hand, the amounts of methanol and ethanol adsorption were just 6.8 and 0.8 $cm^3 g^{-1}$ (even at $P/P_0 = 0.9$), respectively, which were negligible compared to that of water adsorption. These results indicate that **1** selectively adsorbed small water molecules (molecular area: 10.5 $Å^2$) but excluded methanol molecules (17.9 $Å^2$) and ethanol molecules with larger molecular area (23 $Å^2$).

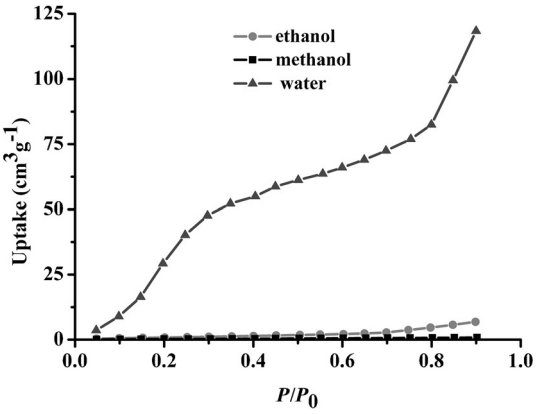

Figure 3. Water, methanol and ethanol adsorption isotherms for compound **1**.

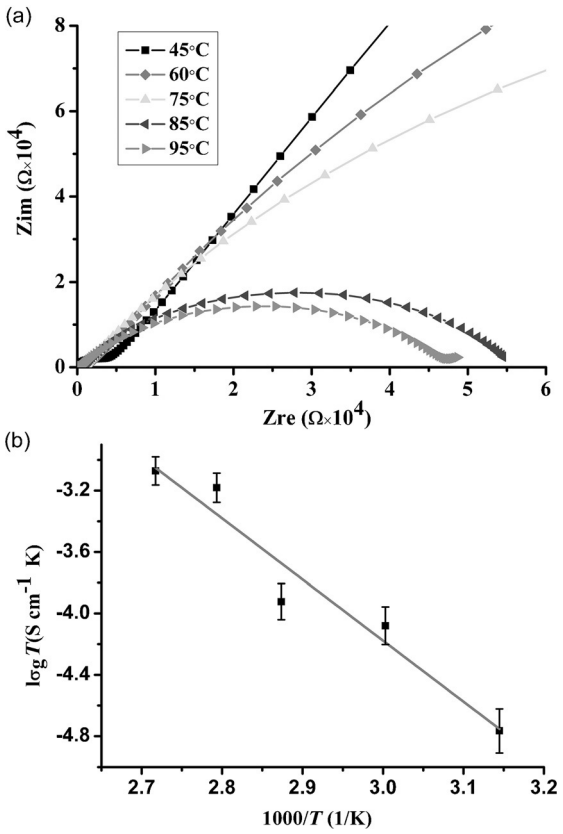

Figure 4. a) Nyquist plot for **1** at different temperatures with 95% RH. b) Arrhenius plots of the conductivity of **1**.

The high chemical stability, the encapsulation of POMs and the many water molecules within the channels prompted us to check the proton-conducting ability of **1**. Besides, the excellent capacity for water adsorption also indicates the good water retention in the framework. The proton conductivities of **1** at a relative humidity (RH) of approximately 95% were evaluated by the ac impedance method by using a compacted pellet of the powdered crystalline sample. The bulk conductivity was evaluated by semicircle fittings of the Nyquist plots (Figure 4a). Figure S8 in the Supporting Information shows the $\log(\sigma$ [$S\,cm^{-1}$]) versus temperature plot at 45–95 °C. The conductivity of **1** increases with increasing temperature from 5.4×10^{-8} $S\,cm^{-1}$ at 45 °C to 1.84×10^{-6} $S\,cm^{-1}$ at 95 °C, which indicated that the proton conductivities strongly depend on temperature. Moreover, there is no structural transformation after the impedance measurement (Figure S9 in the Supporting Information). The enhanced conductivities may be attributed to the fact that the raised temperature accelerates proton transition within channels. The data are plotted in the form of $\log(\sigma T$ [$S\,cm^{-1}\,K$]) versus 1000/*T*, and the linear correlation in the plot is utilized to extract the activation energy (*Ea*) of proton transport (Figure 4b). The activation energy is 0.34 eV ($R^2 = 0.928$), implying that Grotthuss mechanism is dominant for the proton conduction in compound **1**,[12] which is consistent with the architectural feature that Keggin polyanions are pillared into the channel without mobility.

Recently, intense attention has focused on colorimetric biosensing in biological science and analytical chemistry owning to its simplicity, rapidity, cost effectivity and direct visual readout. As **1** has a 3D metal–organic framework pillared by polyoxometalates with redox activity, its peroxidase-like activity was evaluated by the catalytic oxidation of peroxidase substrate TMB in the presence of H_2O_2. As shown in Figure 5, in the absence and presence of H_2O_2, a colorless TMB solution was observed, which displayed a negligible absorption in the range 350 to 800 nm, indicating that no oxidation reaction occurred in the absence of **1**. In contrast when **1** was introduced into the solution, a typical deep-blue color was observed in the reaction mixture, and the solutions exhibited intense characteristic absorbance at 369 and 652 nm. The phenomenon is similar to that observed for the commonly used horseradish peroxidase (HRP) enzyme[9a] and the adsorption bands could be attributed to the charge-transfer complexes derived from the one-electron oxidation of TMB.[13] These results indicate that compound **1** has peroxidase-like catalytic ability and it can catalyze the oxidation of TMB in the presence of H_2O_2. Meanwhile, the structure of **1** can be well retained under the reaction conditions (Figure S10 in the Supporting Information). It is proposed that the nature of the peroxidase-like activity of **1** originates from its catalytic ability to decompose H_2O_2 into $^{\bullet}OH$ radicals through electron transfer.[14] Similar to HRP, the catalytic activity of **1** is dependent on the pH value and H_2O_2 concentration. The optimal pH is 6.0 (Figure S11 in the Supporting Information). Thus, pH 6.0 was adopted as standard for subsequent activity analysis. We also detected the dynamics of

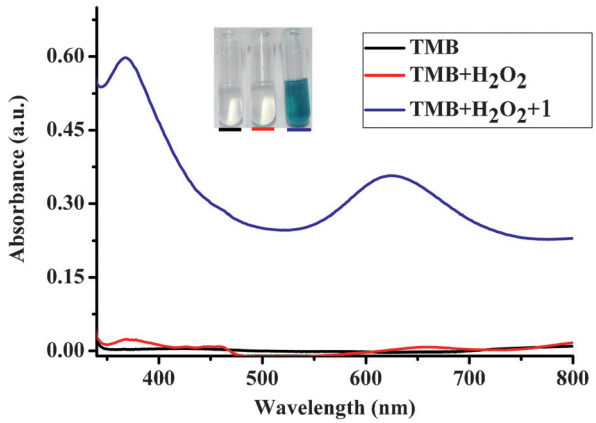

Figure 5. UV/Vis adsorption spectra for TMB, TMB + H_2O_2 and TMB + H_2O_2 + **1** in a pH 6.0 acetate buffer. [TMB]: 0.2 mM, [H_2O_2]: 0.2 mM, [**1**]: 0.03 mg mL^{-1}. Inset: corresponding photographs.

oxidation of TMB to find its time dependence. Compound **1** can catalyze the oxidation of TMB within 1 min and the reaction reached equilibrium after 6 min (Figure S12 in the Supporting Information).

Given the intrinsic peroxidase properties of **1**, a colorimetric method for detection of H_2O_2 using **1**-catalyzed blue color change was established. Since the catalytic activity of MOFs is highly dependent on the concentration of H_2O_2 in solution, the method could be used for the quantitative evaluation of H_2O_2. Figure 6 shows the increase in absorbance at 652 nm upon increasing H_2O_2 concentration in solution. A linear relationship (Figure 6, inset) is observed between the absorbance and the H_2O_2 concentration ranging from 10.0 to 50 μM for **1** ($R^2 = 0.99$) with a detection limit of 1.37 μM.

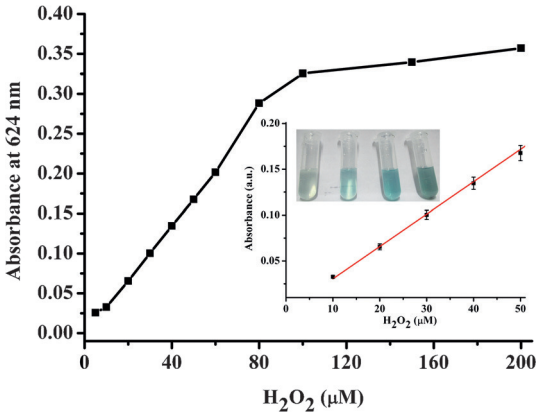

Figure 6. Dose-response curve for H_2O_2 detection using **1** under optimum conditions. Inset: linear calibration plot for H_2O_2 and corresponding photographs of the colored reaction mixtures for different concentrations of H_2O_2.

Conclusion

In conclusion, a new POM-pillared metal organic framework (**1**) has been successfully prepared by hydrothermal method. Moreover, compound **1** exhibits high chemical stability and selective adsorption of water. Crucially, the proton-conducting properties as well as intrinsic peroxidase-like activity for colorimetric assay of H_2O_2 of compound **1** provide the opportunity for practical applications.

Experimental Section

Materials

All reagents for synthesis were purchased from commercial sources and used without further purification

Synthesis of $Cu_6(Trz)_{10}(H_2O)_4[H_2SiW_{12}O_{40}]\cdot 8H_2O$ (1)

A mixture of $Cu(NO_3)_2\cdot 3H_2O$ (36 mg, 0.15 mmol), Trz (42 mg, 0.6 mmol) and $H_4SiW_{12}O_{40}\cdot xH_2O$ (30 mg, 0.015 mmol) was dissolved in 8 mL of distilled water. After the pH of the mixture was adjusted to about 2.0 with 1.0 mol L^{-1} HCl and stirred for 30 min at room temperature, the suspension was put into a Teflon-lined autoclave and kept under autogenous pressure at 160 °C for 3 days. After cooling to room temperature slowly, blue block crystals were filtered and washed with distilled water (yield 64% based on Cu). Elemental analyses calcd (%) for **1**: C 3.90, H 0.97, N 9.10; found: C 3.87, H 0.92, N 9.17. IR (KBr pellet): $\tilde{\nu} = 3441$ (m), 1625 (w), 1458 (w), 1170 (w), 1061 (s), 962 (s), 875 (w), 796 cm^{-1} (s).

Crystal data for 1: $C_{20}H_{44}Cu_6N_{30}O_{52}SiW_{12}$, $Fw = 4128.19$ g mol^{-1}, monoclinic, *C2/c*, $a = 11.926(5)$, $b = 14.419(5)$, $c = 24.311(5)$ Å, $\alpha = 90°$, $\beta = 103.424(5)°$, $V = 4066(2)$ Å^3, $Z = 2$, $T = 293(2)$ K, $R(\text{int}) = 0.0419$, 29764 reflections collected, $\rho_{calcd} = 3.372$ g cm^{-3}, GOF = 1.023 for 15510 reflections with $I > 2\sigma(I)$, $R1 = 0.0644$, $wR2 = 0.1786$ ($I > 2\sigma(I)$). CCDC-1058210 contains the supplementary crystallographic data for this paper. These data can be obtained free of charge from The Cambridge Crystallographic Data Centre via www.ccdc.cam.ac.uk/data_request/cif.

Proton conductivity measurements

The powders were prepared by grinding the sample with a mortar and pestle. With a press and a die measuring 13 mm in diameter and 1.5 mm (±0.08%) in thickness, samples of **1** were pressed into disk-shaped pellets. The impedances were measured with a frequency response analyzer/potentiostat (Princeton Applied Research PAR 2273, EG & GPARC, Princeton, NJ) over a frequency range from 0.1 Hz to 1 MHz, with a quasi-four probe electrochemical cell and an applied ac voltage of 100 mV. Measurements were taken in the temperature range of 45–95 °C with 95% relative humidity (controlled by using an HDHWHS-50 incubator). ZSimpWin software was used to extrapolate impedance data results by means of an equivalent circuit simulation to complete the Niquist plot and obtain the resistance values. Conductivity was calculated using the following equation:

$$\sigma = L/RS$$

where σ is the conductivity [S cm^{-1}], L is the measured sample thickness [cm], S is the electrode area [cm^2] and R is the impedance [Ω].

Detection of H_2O_2 using 1 as peroxidase mimetics

To investigate the peroxidase-like activity of the as-prepared **1**, the catalytic oxidation of the peroxidase substrate TMB in the presence of H_2O_2 was tested. The measurements were carried out by moni-

toring the absorbance change of TMB at 652 nm. In a typical experiment, 20 μL of **1** dispersion stock solution (3 mg mL^{-1}) were mixed in 1.6 mL of NaAc buffer solution (pH 6.0), followed by the addition of 400 μL of TMB solution (1 mM, ethanol solution). Then, 20 μL of H_2O_2 of various concentrations was added into the mixture. The mixed solution was incubated at room temperature for 5 min for standard curve measurement.

Acknowledgements

This work was financially supported by the NSFC of China(No. 21471027, 21171033, 21131001, 21222105), National Key Basic Research Program of China(No. 2013CB834802), The Foundation for Author of National Excellent Doctoral Dissertation of P.R. China(FANEDD) (No. 201022), Changbai Mountain Scholars of Jilin Provinceand FangWu distinguished young scholar of NENU.

Keywords: colorimetric biosensing · metal–organic framework · polyoxometalates · proton conductivity · stability

[1] a) H. C. Zhou, J. R. Long, O. M. Yaghi, *Chem. Rev.* **2012**, *112*, 673; b) M. Yoon, R. Srirambalaji, K. Kim, *Chem. Rev.* **2012**, *112*, 1196; c) J. P. Zhang, Y. B. Zhang, J. B. Lin, X. M. Chen, *Chem. Rev.* **2012**, *112*, 1001; d) J. Liu, L. Chen, H. Cui, J. Zhang, L. Zhang, C. Y. Su, *Chem. Soc. Rev.* **2014**, *43*, 6011; e) T. Zhang, W. Lin, *Chem. Soc. Rev.* **2014**, *43*, 5982; f) Y. He, W. Zhou, G. Qian, B. Chen, *Chem. Soc. Rev.* **2014**, *43*, 5657; g) S. Qiu, M. Xue, G. Zhu, *Chem. Soc. Rev.* **2014**, *43*, 6116; h) Z. Hu, B. J. Deibert, J. Li, *Chem. Soc. Rev.* **2014**, *43*, 5815; i) P. Ramaswamy, N. E. Wong, G. K. H. Shimizu, *Chem. Soc. Rev.* **2014**, *43*, 5913.

[2] a) S. Bureekaew, S. Horike, M. Higuchi, M. Mizuno, T. Kawamura, D. Tanaka, N. Yanai, S. Kitagawa, *Nat. Mater.* **2009**, *8*, 831; b) H. Okawa, M. Sadakiyo, T. Yamada, M. Maesato, M. Ohba, H. Kitagawa, *J. Am. Chem. Soc.* **2013**, *135*, 2256; c) G. K. Shimizu, J. M. Taylor, S. Kim, *Science* **2013**, *341*, 354; d) S. S. Nagarkar, S. M. Unni, A. Sharma, S. Kurungot, S. K. Ghosh, *Angew. Chem. Int. Ed.* **2014**, *53*, 2638; *Angew. Chem.* **2014**, *126*, 2676; e) T. Yamada, K. Otsubo, R. Makiura, H. Kitagawa, *Chem. Soc. Rev.* **2013**, *42*, 6655; f) X. Meng, X. Z. Song, S. Y. Song, G. C. Yang, M. Zhu, Z. M. Hao, S. N. Zhao, H. J. Zhang, *Chem. Commun.* **2013**, *49*, 8483.

[3] a) P. M. Schoenecker, C. G. Carson, H. Jasuja, C. J. J. Flemming, K. S. Walton, *Ind. Eng. Chem. Res.* **2012**, *51*, 6513; b) J. J. Low, A. I. Benin, P. Jakubczak, J. F. Abrahamian, S. A. Faheem, R. R. Willis, *J. Am. Chem. Soc.* **2009**, *131*, 15834; c) S. S. Kaye, A. Dailly, O. M. Yaghi, J. R. Long, *J. Am. Chem. Soc.* **2007**, *129*, 14176.

[4] a) T. Yamase, *Chem. Rev.* **1998**, *98*, 307; b) A. Müller, F. Peters, M. T. Pope, G. Gatteschi, *Chem. Rev.* **1998**, *98*, 239; c) H. N. Miras, J. Yan, D. L. Long, L. Cronin, *Chem. Soc. Rev.* **2012**, *41*, 7403; d) S. T. Zheng, G. Y. Yang, *Chem. Soc. Rev.* **2012**, *41*, 7623; e) J. Hao, Y. Xia, L. Wang, L. Ruhlmann, Y. Zhu, Q. Li, P. Yin, Y. Wie, H. Guo, *Angew. Chem. Int. Ed.* **2008**, *47*, 2626; *Angew. Chem.* **2008**, *120*, 2666; f) Y. Yang, B. Zhang, Y. Wang, L. Yue, W. Li, L. Wu, *J. Am. Chem. Soc.* **2013**, *135*, 14500.

[5] a) D. Y. Du, J. S. Qin, S. L. Li, Z. M. Su, Y. Q. Lan, *Chem. Soc. Rev.* **2014**, *43*, 4615; b) C. Y. Sun, S. X. Liu, D. D. Liang, K. Z. Shao, Y. H. Ren, Z. M. Su, *J. Am. Chem. Soc.* **2009**, *131*, 1883; c) F. J. Ma, S. X. Liu, C. Y. Sun, D. D. Liang, G. J. Ren, F. Wei, Y. G. Chen, Z. M. Su, *J. Am. Chem. Soc.* **2011**, *133*, 4178; d) C. Duan, M. Wei, G. Guo, C. He, Q. Meng, *J. Am. Chem. Soc.* **2010**, *132*, 3321; e) Q. Han, C. He, M. Zhao, B. Bi, J. Niu, C. Duan, *J. Am. Chem. Soc.* **2013**, *135*, 10186; f) B. Nohra, H. E. Moll, L. M. R. Albelo, P. Mialane, J. Marrot, C. Mellot-Draznieks, M. O'Keeffe, R. N. Biboum, J. Lemaire, B. Keita, L. Nadjo, A. Dolbecq, *J. Am. Chem. Soc.* **2011**, *133*, 13363; g) H. Fu, C. Qin, Y. Lu, Z. M. Zhang, Y. G. Li, Z. M. Su, W. L. Li, E. B. Wang, *Angew. Chem. Int. Ed.* **2012**, *51*, 7985; *Angew. Chem.* **2012**, *124*, 8109.

[6] a) X. Kuang, X. Wu, R. Yu, J. P. Donahue, J. Huang, C. Z. Lu, *Nat. Chem.* **2010**, *2*, 461; b) X. L. Wang, Y. G. Li, Y. Lu, H. Fu, Z. M. Su, E. B. Wang, *Cryst. Growth Des.* **2010**, *10*, 4227; c) Y. Q. Lan, S. L. Li, J. F. Qin, D. Y. Du, X. L. Wang, Z. M. Su, Q. Fu, *Inorg. Chem.* **2008**, *47*, 10600; d) X. L. Wang, Y. F. Wang, G. C. Liu, A. X. Tian, J. W. Zhang, H. Y. Lin, *Dalton Trans.* **2011**, *40*, 9299.

[7] a) Z. X. Zhang, Z. J. Wang, X. L. Wang, X. R. Yang, *Sens. Actuators B* **2010**, *147*, 428; b) J. Wang, X. Mi, H. Guan, X. Wang, Y. Wu, *Chem. Commun.* **2011**, *47*, 2940; c) J. Yin, H. Cao, Y. Lu, *J. Mater. Chem.* **2012**, *22*, 527.

[8] a) L. Z. Gao, J. Zhuang, L. Nie, J. B. Zhang, Y. Zhang, N. Gu, T. H. Wang, J. Feng, D. L. Yang, S. Perrett, X. Yan, *Nat. Nanotechnol.* **2007**, *2*, 577; b) Z. Dai, S. Liu, J. Bao, H. Ju, *Chem. Eur. J.* **2009**, *15*, 4321; c) A. Asati, S. Santra, C. Kaittanis, S. Nathand, J. M. Perez, *Angew. Chem. Int. Ed.* **2009**, *48*, 2308; *Angew. Chem.* **2009**, *121*, 2344; d) Y. Song, K. Qu, C. Zhao, J. Ren, X. Qu, *Adv. Mater.* **2010**, *22*, 2206; e) Y. J. Long, Y. F. Li, Y. Liu, J. J. Zheng, J. Tang, C. Z. Huang, *Chem. Commun.* **2011**, *47*, 11939; f) Y.-L. Dong, H.-G. Zhang, Z. U. Rahman, L. Su, X.-J. Chen, J. Hu, X.-G. Chen, *Nanoscale* **2012**, *4*, 3969.

[9] a) D. Feng, Z.-Y. Gu, J.-R. Li, H.-L. Jiang, Z. Wie, H.-C. Zhou, *Angew. Chem. Int. Ed.* **2012**, *51*, 10307; *Angew. Chem.* **2012**, *124*, 10453; b) X. Zhu, H. Zheng, X. Wei, Z. Lin, L. Guo, B. Qiu, G. Chen, *Chem. Commun.* **2013**, *49*, 1276; c) L. Ai, L. Li, C. Zhang, J. Fu, J. Jiang, *Chem. Eur. J.* **2013**, *19*, 15105; d) J.-W. Zhang, H.-T. Zhang, Z.-Y. Du, X. Wang, S.-H. Yu, H. L. Jiang, *Chem. Commun.* **2014**, *50*, 1092; e) H.-T. Zhang, J.-W. Zhang, G. Huang, Z.-Y. Du, H. L. Jiang, *Chem. Commun.* **2014**, *50*, 12069; f) W. Dong, X. Liu, W. Shi, Y. Huang, *RSC Adv.* **2015**, *5*, 17451.

[10] A. Spek, *J. Appl. Crystallogr.* **2003**, *36*, 7.

[11] a) S. Uchida, N. Mizuno, *J. Am. Chem. Soc.* **2004**, *126*, 1602; b) R. Kawamoto, S. Uchida, N. Mizuno, *J. Am. Chem. Soc.* **2005**, *127*, 10560; c) Z. M. Zhang, S. Yao, Y. G. Li, R. Clérac, Y. Lu, Z. M. Su, E. B. Wang, *J. Am. Chem. Soc.* **2009**, *131*, 14600; d) S. G. Mitchell, C. Streb, H. N. Miras, D. Boyd, D. L. Long, L. Cronin, *Nat. Chem.* **2010**, *2*, 308.

[12] K. D. Kreuer, A. Rabenau, W. Weppner, *Angew. Chem. Int. Ed. Engl.* **1982**, *21*, 208; *Angew. Chem.* **1982**, *94*, 224.

[13] a) P. D. Josephy, T. Eling, R. P. Mason, *J. Biol. Chem.* **1982**, *257*, 3669; b) X. Sun, S. Guo, C.-S. Chung, W. Zhu, S. Sun, *Adv. Mater.* **2013**, *25*, 132.

[14] a) X.-Q. Zhang, S.-W. Gong, Y. Zhang, T. Yang, C.-Y. Wang, N. Gu, *J. Mater. Chem.* **2010**, *20*, 5110; b) Y. Chen, H. Cao, W. Shi, H. Liu, Y. Huang, *Chem. Commun.* **2013**, *49*, 5013.

Received: April 18, 2015
Published online on July 14, 2015

